Int. J. Heat Mass Transfer. Vol. 8, pp. 781–791. Pergamon Press 1965. Printed in Great Britain

THE BREAKDOWN OF THE LIQUID FILM IN ANNULAR TWO-PHASE FLOW

G. F. HEWITT and P. M. C. LACEY†
Atomic Energy Research Establishment, Harwell, Berkshire

(*Received* 4 *January* 1964 *and in revised form* 9 *November* 1964)

Abstract—The breakdown of liquid films may be the cause of burnout in the higher quality regimes of two-phase steam–water flow. An investigation of the breakdown of the liquid film in air–water annular flow is reported, which shows that the films can exist in a metastable state and will not break down unless there is an external disturbance. If such a disturbance is provided in the form of a dry patch on the solid surface then the minimum water flow rate at which the patch will be re-wetted decreases as the velocity of the gas phase increases.

NOMENCLATURE

d_{e1}, equivalent diameter, inner region [ft];
d_{e2}, equivalent diameter, outer region [ft];
F_1, friction factor, inner region [dimensionless];
F_2, friction factor, outer region [dimensionless];
k, von Kármán constant [dimensionless];
m, film thickness [ft];
m_r, relative film thickness [ft];
dp/dl, pressure gradient [pdl/ft^2 ft];
r_m, radius of maximum velocity, or zero shear [ft];
r_{01}, radius of core rod [ft];
r_{02}, inside radius of tube [ft];
Re_1, Reynolds number in inner region [dimensionless];
Re_2, Reynolds number in outer region [dimensionless];
u, velocity in liquid film [ft/s];
u^*, liquid friction velocity $[\sqrt{(\tau_{02}/\rho_L)}]$ [ft/s];
u^+, velocity parameter (u/u^*) [dimensionless];
U_1, mean velocity in inner region [ft/s];
U_2, mean velocity in outer region [ft/s];
$\bar{U}$, overall mean velocity in channel [ft/s];
W_{LF}, mass flow rate of liquid in film [lb/s];
W^+, mass flow rate parameter $(W_{LF}/2\pi r_{02}\mu_L)$ [dimensionless];
y, distance from wall [ft];
y^+, distance parameter $(u^* y\rho_L/\mu_L)$ [dimensionless];
y_i^+, dimensionless film thickness;
$(y_i^+)_c$, critical value of y_i^+;
ϵ, roughness height [ft];
θ, contact angle [degrees];
μ_L, liquid viscosity [lb/ft s];
ρ_L, liquid density [lb/ft^3];
σ, liquid surface tension [pdl/ft];
τ_{01}, shear stress on inner surface [pdl/ft^2];
τ_{02}, shear stress on outer surface [pdl/ft^2];

1. INTRODUCTION

IN EVAPORATIVE heat transfer to two-phase single component mixtures (for example, steam and water), a critical heat flow is observed, above which a less efficient regime of heat transfer takes over. This transition is commonly referred to as the "burnout", or "dry-out", heat flux. At higher quality,‡ the regime of flow is often annular; the liquid flows partly in the form of a film on the channel wall and partly as droplets entrained in the gas phase. In this flow regime, the critical heat flux almost certainly corresponds to the breakdown of the liquid film on the heater surface. The film would, of course, disappear when all the liquid flowing in it had been evaporated away, but breakdown may occur before complete evaporation.

† Present address: Department of Chemical Engineering, University of Exeter, Exeter, Devon.

‡ "Quality" here refers to the ratio of the vapor phase mass flow rate to the total mass flow rate.

Hartley and Murgatroyd [1] have considered the stability of a flowing film in terms of two criteria, based respectively on a force balance at a dry patch and on energy flow considerations. The two approaches yield rather similar results except that the force balance criterion depends strongly on the wetting angle; in the present paper we shall confine attention to this case.

Hartley and Murgatroyd dealt with a number of types of film flow and particularly with annular flow in which the film's motion was caused by surface shear only. For any given system, their theory indicates that the "minimum wetting rate", i.e. the minimum liquid flow rate required to re-wet the surface after the formation of a dry patch, decreases with increasing gas rate.

It may be noted that the existence of a dry patch is an essential condition in the above-mentioned analysis; if the surface is already wetted, then the flow rate could quite possibly be reduced below the "minimum wetting rate" without breakdown of the film. The film in this latter case would be metastable and some mechanism for breaking it down would be required. This point will be returned to below.

The object of the experiments to be described was to investigate the film breakdown phenomenon under carefully controlled experimental conditions and to provide data for quantitative comparatison with the theoretical studies.

2. EXPERIMENTAL

The experiments were carried out with air/water flow at room temperature and at pressures slightly above atmospheric. The air and water supply system was similar to that previously described elsewhere [2, 3, etc.]; air was derived from the site main and metered by an orifice plate and water was recirculated by a centrifugal pump and metered with Rotameters.

Film breakdown was studied by artificially producing a dry patch using an air jet directed at the wall of the flow tube, and the apparatus used in the initial experiments is sketched in Fig. 1.

Air was fed in through the bottom of the 1¼ in bore acrylic resin flow tube and passed through a calming length of several feet before meeting the water, which entered the tube smoothly through a porous wall section, A. A dry patch was made in the liquid film on the tube wall by simply blowing air through the capillary tube B. The air jet was then turned off and the subsequent behaviour of the dry patch was studied. The object was to reduce the liquid flow rate in successive trials until the dry patch became permanent; it was found, however, that long before the liquid flow had been reduced to the point where it failed to re-cover the dry patch,

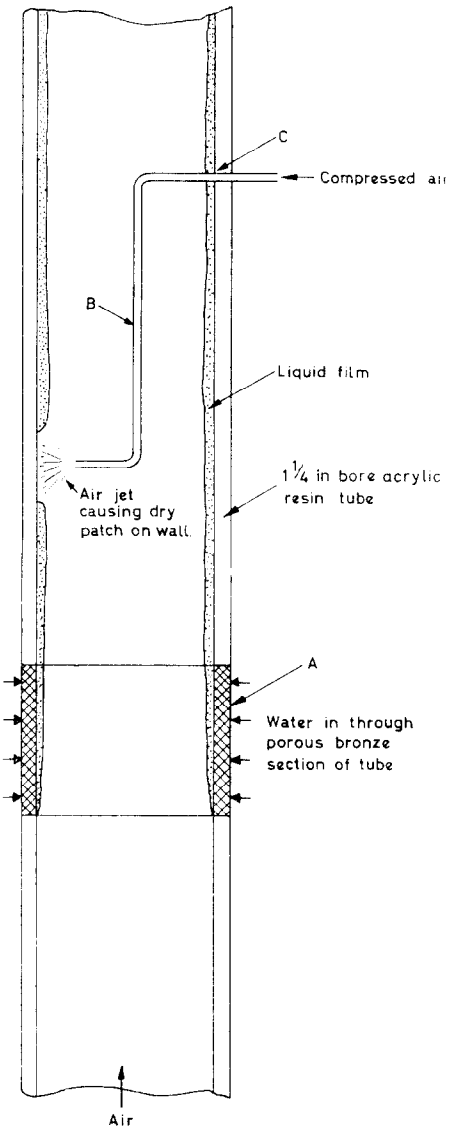

FIG. 1. Flow tube diagram for initial experiments.

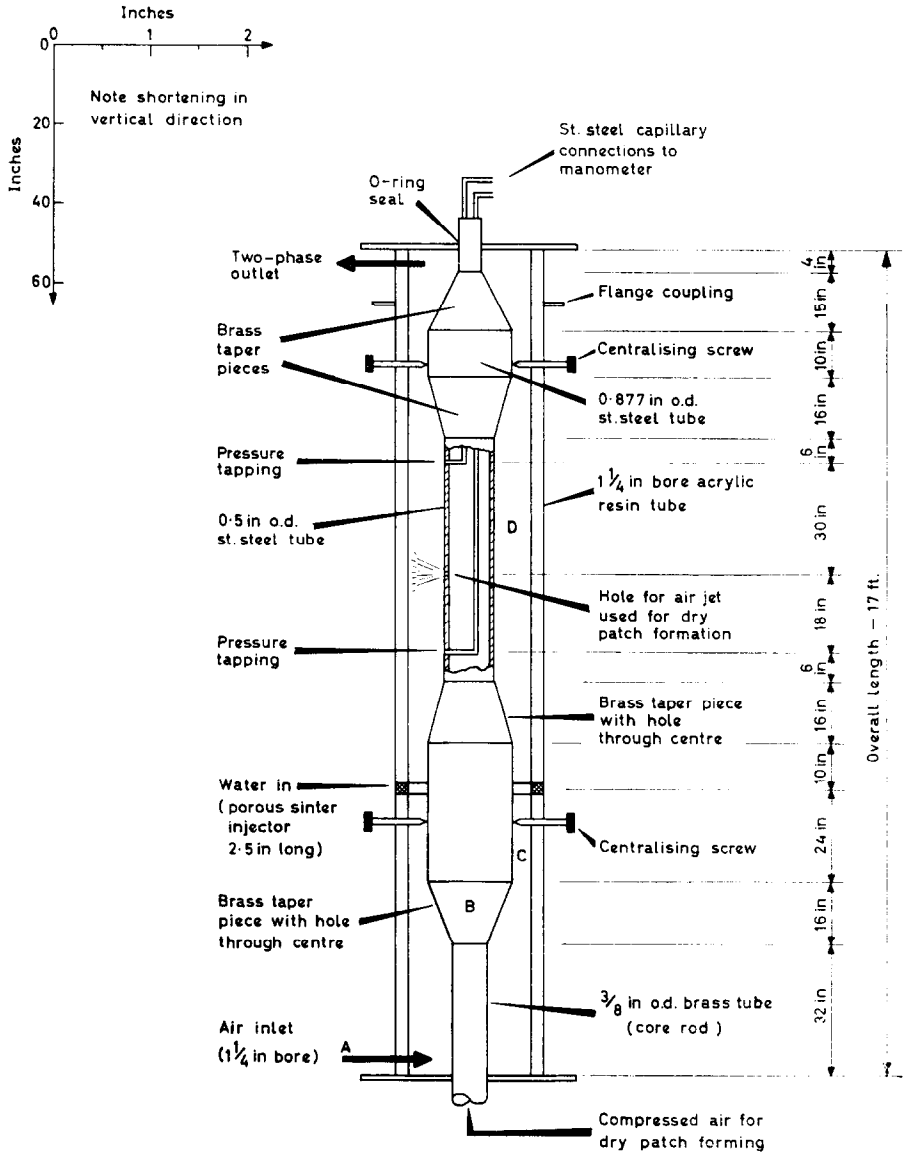

FIG. 2. Variable area flow channel.

breakdown started to occur at the injector and also at point C where the air-jet tube entered the flow tube. The initial method was therefore abandoned and a new one sought.

The experimental arrangement finally used is shown in Fig. 2. (For space reasons, very different scales have been used in the vertical and horizontal directions, in the ratio of 25:1). This arrangement depended for its effectiveness on the assumption that the Hartley–Murgatroyd theory was valid, in that at higher air velocities the surface would be more easily wetted.

A climbing film was made to form as above, on the wall of a $1\frac{1}{4}$ in bore acrylic resin flow tube, but in the modified test section the air was accelerated at the liquid injection point to stabilize the film in this rather sensitive area. The air was then decelerated before entry to the

region of the tube used for the stability tests, and then accelerated again at the outlet. This variation in gas velocity was achieved by using a variable cross-section metal core in the centre of the flow tube.

After entering the channel through a tee-piece at A, the air flowed through a 32-in annular calming section $1\frac{1}{4}$ in o.d. by $\frac{3}{8}$ in i.d., and then gradually accelerated as it flowed past the very gently tapered section of the core at B. In the annular space, C, which was 3 ft long, the water was injected at a point about 2 ft from the entrance, to form a film on the inner surface of the outer wall. At the low water rates being employed in these experiments the entrainment was minimal and the liquid remained substantially in the film; the core therefore remained dry. The water injector used was of the porous sinter type and was an improved version of the described previously [4], particular care being taken to ensure circumferential uniformity of flow.

At the end of section C the air was reduced in velocity by a factor of about 1·7 by tapering the core down to $\frac{1}{2}$ in diameter, and the next 5 ft of that channel (D) were used for the stability tests; this portion will in future be referred to as the "test section". The air was then accelerated again to provide a stable film at the outlet. In the "test section" region a hole was drilled in the wall of the core tube to allow a jet of air to be blown on to the climbing film on the flow tube, to provide the dry patch. The air for this was supplied via the bottom end of the core tube.

It is essential in the theoretical analysis to have data on pressure gradient in the test section, and pressure and pressure difference measurements were made by means of stainless steel capillary tubes soldered into the core tube wall. The ends of these tubes were ground down flush with the core tube surface and the whole of the core was carefully polished, particular care being taken to avoid roughnesses at the joins between the tapered and straight sections. Satisfactory concentricity of the core and the flow tube at the test section was obtained by manipulation of the centering screws and the top and bottom flanges.

The procedure adopted was to set the required air flow rate, and a liquid rate well above the minimum wetting rate, and to reduce the liquid rate in stages. For each liquid flow rate, the pressure drop was measured and a dry patch formed by flowing. If the dry patch was rewetted on cessation of the air jet, the liquid rate was reduced again and the procedure repeated. Once the minimum wetting rate had been reached, the liquid flow rate was first increased, to re-wet the surface, and then was further reduced in small steps until the film broke down spontaneously (i.e. without the artificial formation of a dry patch) and the rate at spontaneous breakdown was noted.

3. RESULTS

The results of the minimum wetting rate measurements are shown in Fig. 3. The water rate was reduced by approximately 2 lb/h for each successive dry patch test. Each minimum wetting rate, therefore, falls between two limits;

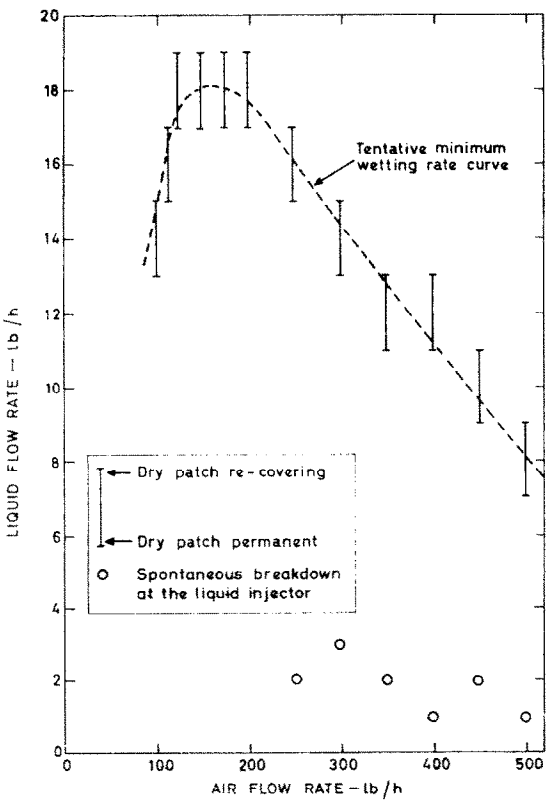

FIG. 3. De-wetting experimental data.

at the upper the surface is re-wetted and at the lower the dry patch is permanent. No attempt was made to obtain a more precise figure for minimum wetting rate and the results are plotted as bar-lines between the two limits. It will be observed that in the higher gas rate region the minimum wetting rate does decrease with increase in gas rate, in agreement with the Hartley and Murgatroyd theory. At lower gas rates, however, the minimum wetting rate passes through a maximum and begins to decrease with decreasing gas rate. This latter trend is also to be expected, since the boundary between the climbing film and churn flow regimes is being approached (see reference 6 for map of regimes); at lower water flow rates this regime boundary is independent of water rate, and near the boundary it is possible [6] to have a film of liquid maintained in an equilibrium state on the tube wall with no net feed of water into it: in this extreme case, therefore, the minimum wetting rate is zero.

The form the dry-patch took was interesting; at water rates above the minimum wetting rate the patch was more or less circular. The re-wetting of the surface took place in a complex manner, usually by splitting of the dry patch by rivulets, followed by the erosion of the ends and sides of the resultant secondary patches. The time required for re-wetting increased as the water flow rate decreased; this increase in patch life-time was rapid as the minimum wetting rate was approached. The initial patch was about $\frac{1}{2}$ in diameter. When, on the other hand, a dry patch was formed at water rates below the minimum wetting rate, a dry streak was often formed downstream of the drying point. This streaking effect was most pronounced at the higher air flow rates.

It will be seen from the lower part of Fig. 3 that the flow rate for spontaneous breakdown of the liquid film is of the order of 2 lb/h, i.e. very much lower than the minimum wetting rate. Even then, breakdown started at the water injector; in no case was true spontaneous breakdown observed, i.e. within the film.

The pressure gradient data are plotted in Fig. 4; they show a self-consistent increase with both air and water flow rate. Pressure gradient, flow rate and physical property data are included in Table 1.

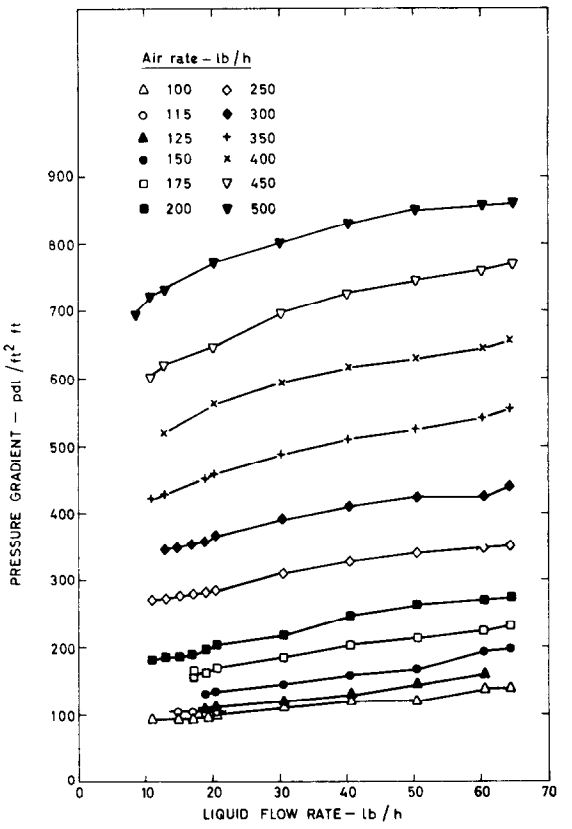

FIG. 4. Pressure drop data.

4. ANALYSIS AND DISCUSSION

The analysis of the data from the present experiments was carried out on the Harwell *Mercury* computer. Using the notation of the present paper we may write Hartley and Murgatroyd's equations (29), (30) and (31), [1], based on the von Kármán universal velocity profile, as:

$$\frac{2\sigma(1-\cos\theta)}{\mu_L u^*} = \frac{(y_i^+)_c^3}{3} \text{ for } (y_i^+)_c < 5 \quad (1)$$

$$\frac{2\sigma(1-\cos\theta)}{\mu_L u^*} = 25\,(y_i^+)_c \ln^2 (y_i^+)_c - 80{\cdot}5\,(y_i^+)_c \ln (y_i^+)_c + 89{\cdot}8\,(y_i^+)_c - 82{\cdot}3, \quad (2)$$

$$\text{for } 5 < (y_i^+)_c < 30$$

$$\frac{2\sigma(1-\cos\theta)}{\mu_L u^*} = 6{\cdot}25\,(y_i^+)_c \ln^2 (y_i^+)_c + 15\,(y_i^+)_c \ln (y_i^+)_c + 15{\cdot}25\,(y_i^+)_c - 1084, \quad (3)$$

$$\text{for } (y_i^+)_c > 30$$

where u^+ and y^+ are defined by $u^+ = u/u^*$ and $y^+ = u^* y \rho_L/\mu_L$, and where u^* (the friction velocity), is defined as $\sqrt{(\tau_{02}/\rho_L)}$. μ_L is the liquid viscosity and τ_{02} the shear stress at the wall.

The first aim was to calculate for a given gas and liquid rate the appropriate values of u^* and y^+ for insertion into equations (1) to (3).

If the assumption of constant shear stress throughout the liquid film is made, the dimensionless film thickness, y_i^+, can be calculated from the dimensionless film flow rate W^+ which is defined by:

$$W^+ = \frac{W_{LF}}{2\pi r_{02}\mu_L} = \int_0^{y_i^+} u^+ \,\mathrm{d}y^+ \quad (4)$$

where W_{LF} is the mass rate of flow in the film (lb/s), r_{02} is the tube radius (ft) and μ_L the liquid viscosity (lb/ft s). By insertion of the u^+ vs y^+ relationships given by the von Kármán equations [equations 25(a), (b) and (c) of reference 1, with W replaced by u] and integrating, the following equations are obtained for the relation between W^+ and y_i^+:

$$W^+ = 0{\cdot}5\,(y_i^+)^2 \quad \text{for } y_i^+ < 5, \quad (W^+ < 12{\cdot}5) \quad (5)$$

$$W^+ = 12{\cdot}5 + 5\,y_i^+ \ln (y_i^+/5) \quad (6)$$

$$\text{for } 5 < y_i^+ < 30, \ (12{\cdot}5 < W^+ < 281{\cdot}89)$$

$$W^+ = -63{\cdot}61 + 3{\cdot}05\,y_i^+ + 2{\cdot}5\,y_i^+ \ln y_i^+, \quad (7)$$

$$\text{for } y_i^+ > 30, \quad (W^+ > 281{\cdot}89)$$

The value of W^+ is obtained simply from the first part of equation (4), and y_i^+ evaluated by solution of equation (5), (6) or (7). In the case of equations (6) and (7) this solution is obtained iteratively. Values of W^+ and y_i^+ for each condition at which pressure drop was measured are listed in Table 1 (columns 20 and 21).

The next stage in the analysis is the determination of u^* $[=\sqrt{(\tau_{02}/\rho_L)}]$. This determination is not simple since the flow channel has one smooth surface (the core rod) and one of variable roughness (i.e. the liquid film surface). A method for analysing pressure drop data in such channels has been developed recently and is described in more detail elsewhere [7]. In this analytical method, the channel is divided up into two regions bounded by the plane of maximum velocity (or zero shear) and by the respective channel walls in the manner developed by Hall [8]. This is illustrated in Fig. 5. Equivalent

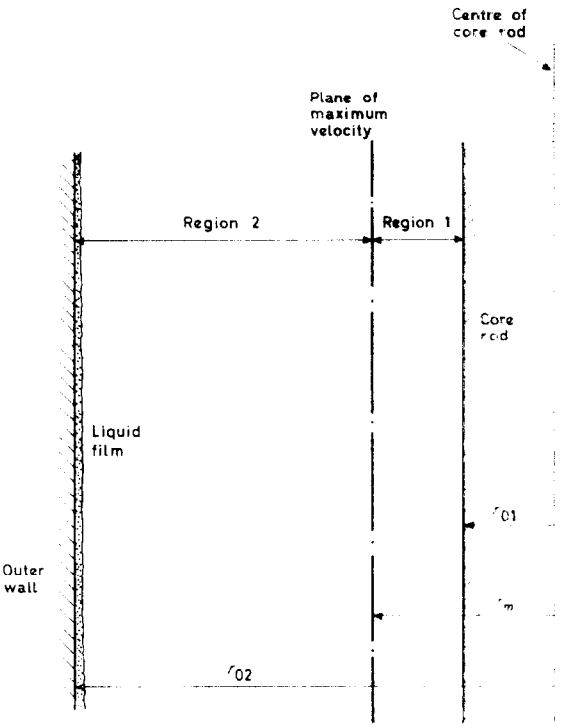

FIG. 5. Regions of flow channel.

diameters, Reynolds numbers and friction factors are defined for the two regions as follows [7]:

$$d_{e1} = \frac{2\,(r_m^2 - r_{01}^2)}{r_{01}}, \quad d_{e2} = \frac{2\,(r_{02}^2 - r_m^2)}{r_{02}} \quad (8, 9)$$

$$Re_1 = \frac{U_1\, d_{e1}\, \rho_G}{\mu_G}, \quad Re_2 = \frac{U_2\, d_{e2}\, \rho_G}{\mu_G} \quad (10, 11)$$

$$F_1 = \frac{\tau_{01}}{\rho_G U_1^2} = \frac{(\mathrm{d}p/\mathrm{d}l)\,.\,(d_{e1}/4)}{\rho_G U_1^2},$$

$$F_2 = \frac{\tau_{02}}{\rho_G U_2^2} = \frac{(\mathrm{d}p/\mathrm{d}l)\,.\,(d_{e2}/4)}{\rho_G U_2^2} \quad (12, 13)$$

Table 1. Experimental data and transformations

Column 1	2	3	4	5	6	7	8	9	10	11	12	13	14	15	16	17	18	19	20	21	22	23	24	25	26	27
Test number	Air rate (lb/h)	Water rate (lb/h)	Air density (lb/ft³)	Air viscosity (lb/ft h)	Water density (lb/ft³)	Water viscosity (lb/ft h)	Pressure gradient (pdl/ft² ft)	$10^3 \times V_m$ (ft)	$10^2 \times d_{e1}$ (ft)	$10^2 \times d_{e2}$ (ft)	U_1 (ft/s)	U_2 (ft/s)	U_1/U_2	$10^{-3} \times Re_1$	$10^{-3} \times Re_2$	$10^3 \times F_1$	$10^3 \times F_2$	ϵ/d_{e2}	w^-	y^+	u^* (ft/s)	$10^4 \times m$ (ft)	$\frac{mg\rho}{\tau_{02}}$	m/d_{e2}	$\frac{m}{d_{e2}} - \frac{5}{Re_2\sqrt{F_2}}$	θ (deg)
1	100	64·5	0·0736	0·0436	62·33	2·499	143	2·72	2·937	7·639	60·40	50·81	1·189	10·77	23·55	3·906	14·36	0·1228	78·49	13·39	0·209	7·127	0·5232	0·00933	0·00756	42·3
2	100	60·5	0·0736	0·0436	62·33	2·499	140	2·73	2·975	7·624	60·22	50·82	1·185	10·87	23·51	3·896	14·03	0·1179	73·63	12·90	0·207	6·944	0·5217	0·00911	0·00731	40·2
3	100	50·5	0·0735	0·0436	62·33	2·499	123	2·78	3·223	7·525	59·35	51·02	1·163	11·60	23·28	3·830	12·10	0·0902	61·46	11·62	0·193	6·714	0·5817	0·00892	0·00697	34·1
4	100	40·5	0·0734	0·0436	62·33	2·499	123	2·78	3·226	7·524	59·41	51·08	1·163	11·61	23·28	3·829	12·09	0·0900	49·29	10·25	0·193	5·925	0·5134	0·00788	0·00592	29·2
5	100	30·5	0·0733	0·0436	62·33	2·499	113	2·81	3·402	7·453	58·36	51·20	1·150	12·11	23·08	3·787	10·97	0·0746	37·12	8·77	0·184	5·312	0·5058	0·00713	0·00506	23·2
6	100	20·5	0·0731	0·0436	62·33	2·499	102	2·85	3·628	7·364	58·28	51·39	1·134	12·75	22·82	3·731	9·73	0·0583	24·95	7·10	0·174	4·556	0·4863	0·00619	0·00397	17·0
7	100	19·0	0·0729	0·0436	62·33	2·499	99	2·86	3·704	7·334	58·21	51·54	1·129	12·97	22·74	3·715	9·38	0·0539	23·12	6·83	0·171	4·454	0·4919	0·00607	0·00380	15·9
8	100	17·0	0·0728	0·0436	62·33	2·499	94	2·89	3·831	7·283	57·94	51·64	1·122	13·34	22·59	3·688	8·82	0·0470	20·69	6·45	0·166	4·332	0·5074	0·00595	0·00359	14·4
9	100	15·0	0·0728	0·0436	62·33	2·499	94	2·89	3·831	7·283	57·94	51·64	1·122	13·34	22·59	3·688	8·82	0·0470	18·25	6·05	0·166	4·065	0·4761	0·00558	0·00323	13·2
10	100	11·0	0·0728	0·0436	62·33	2·499	92	2·90	3·885	7·261	57·80	51·65	1·119	13·49	22·53	3·678	8·61	0·0444	13·39	5·17	0·164	3·520	0·4225	0·00485	0·00245	10·4
11	115	20·5	0·0727	0·0437	62·32	2·465	105	2·95	4·171	7·148	61·61	59·52	1·102	16·39	25·49	3·498	7·28	0·0299	25·29	7·15	0·174	4·528	0·4837	0·00634	0·00404	17·0
12	115	19·0	0·0727	0·0437	62·32	2·465	105	2·95	4·171	7·148	65·61	59·52	1·102	16·39	25·49	3·498	7·28	0·0299	23·44	6·87	0·174	4·353	0·4649	0·00609	0·00379	16·1
13	115	17·0	0·0727	0·0437	62·32	2·465	105	2·95	4·171	7·148	65·61	59·52	1·102	16·39	25·49	3·498	7·28	0·0299	20·97	6·49	0·174	4·111	0·4391	0·00575	0·00345	14·8
14	115	15·0	0·0727	0·0437	62·32	2·465	105	2·95	4·171	7·148	65·61	59·52	1·102	16·39	25·49	3·498	7·28	0·0299	18·51	6·09	0·174	3·856	0·4119	0·00539	0·00309	13·5
15	125	60·5	0·0740	0·0437	62·32	2·465	162	2·81	3·423	7·445	72·46	63·38	1·143	15·12	28·78	3·570	10·14	0·0639	74·64	13·00	0·220	6·495	0·4317	0·00872	0·00700	41·6
16	125	50·5	0·0736	0·0437	62·32	2·465	145	2·86	3·685	7·341	71·86	63·79	1·127	16·06	28·40	3·156	8·88	0·0481	62·30	11·71	0·207	6·225	0·4688	0·00848	0·00661	35·5
17	125	40·5	0·0734	0·0437	62·32	2·465	130	2·91	3·961	7·231	71·18	64·04	1·111	17·05	28·01	3·463	7·81	0·0356	49·97	10·33	0·194	5·844	0·4984	0·00808	0·00606	29·4
18	125	30·5	0·0732	0·0437	62·32	2·465	120	2·95	4·181	7·144	70·76	64·28	1·101	17·84	27·69	3·423	7·09	0·0280	37·63	8·83	0·185	5·233	0·4894	0·00733	0·00518	23·5
19	125	20·5	0·0730	0·0437	62·32	2·465	107	3·01	4·518	7·009	70·13	64·55	1·086	19·06	27·21	3·367	6·17	0·0192	25·29	7·15	0·174	4·529	0·4842	0·00646	0·00412	17·0
20	125	19·0	0·0730	0·0437	62·32	2·465	107	3·01	4·518	7·009	70·13	64·55	1·086	19·06	27·21	3·367	6·17	0·0192	23·44	6·87	0·174	4·354	0·4654	0·00621	0·00387	16·1
21	150	64·5	0·0762	0·0437	62·32	2·465	199	2·84	3·599	7·375	33·46	73·97	1·128	18·86	34·25	3·375	8·80	0·0473	79·58	13·50	0·243	6·114	0·3340	0·00829	0·00673	45·9
22	150	60·5	0·0761	0·0437	62·32	2·465	194	2·86	3·662	7·350	83·32	74·08	1·125	19·13	34·14	3·363	8·54	0·0414	74·64	13·00	0·239	5·973	0·3358	0·00813	0·00654	43·5
23	150	50·5	0·0753	0·0437	62·32	2·465	166	2·93	4·079	7·184	82·69	74·98	1·103	20·93	33·42	3·288	7·04	0·0278	62·30	11·71	0·219	5·881	0·3953	0·00819	0·00640	36·5
24	150	40·5	0·0751	0·0437	62·32	2·465	159	2·95	4·204	7·134	82·53	75·21	1·097	21·47	33·21	3·267	6·67	0·0242	49·97	10·33	0·213	5·320	0·3759	0·00746	0·00561	30·8
25	150	30·5	0·0748	0·0437	62·32	2·465	146	3·00	4·460	7·032	82·3	75·58	1·087	22·58	32·77	3·226	6·00	0·0181	37·63	8·83	0·203	4·782	0·3734	0·00680	0·00483	24·6
26	150	20·5	0·0744	0·0437	62·32	2·465	135	3·04	4·717	6·930	81·92	76·06	1·077	23·70	32·32	3·188	5·43	0·0134	25·29	7·15	0·194	4·055	0·3475	0·00585	0·00375	18·0
27	150	19·0	0·0744	0·0437	62·32	2·465	130	3·06	4·845	6·879	81·64	76·10	1·073	24·26	32·10	3·173	5·19	0·0116	23·44	6·87	0·189	3·988	0·3575	0·00579	0·00579	16·8
28	175	17·1	0·0760	0·0437	62·32	2·465	159	3·09	5·000	6·817	92·86	87·08	1·066	29·06	37·15	3·034	4·71	0·0085	21·10	6·51	0·209	3·431	0·2537	0·00503	0·00307	16·3
29	175	64·5	0·0785	0·0437	62·32	2·465	233	2·88	3·788	7·300	93·55	83·89	1·115	22·91	39·59	3·214	7·70	0·0349	79·58	13·50	0·261	5·680	0·2677	0·00778	0·00634	47·7
30	175	60·5	0·0780	0·0437	62·32	2·465	225	2·90	3·891	7·259	93·71	84·43	1·110	23·43	39·39	3·196	7·34	0·0311	74·64	13·00	0·256	5·581	0·2739	0·00769	0·00621	45·1
31	175	50·5	0·0776	0·0437	62·32	2·465	212	2·93	4·059	7·192	93·55	84·91	1·102	24·28	39·05	3·168	6·81	0·0257	62·30	11·71	0·247	5·201	0·2735	0·00723	0·00568	38·9
32	175	40·5	0·0772	0·0437	62·32	2·465	202	2·95	4·205	7·134	93·52	85·38	1·095	25·02	38·76	3·145	6·40	0·0218	49·97	10·33	0·240	4·720	0·2620	0·00662	0·00500	32·8
33	175	30·5	0·0768	0·0437	62·32	2·465	186	3·00	4·458	7·033	93·20	85·91	1·085	26·30	38·25	3·106	5·77	0·0163	37·63	8·83	0·229	4·236	0·2596	0·00602	0·00430	26·1
34	175	20·5	0·0765	0·0437	62·32	2·465	173	3·04	4·693	6·940	92·91	86·32	1·076	27·49	37·77	3·072	5·26	0·0134	25·29	7·15	0·220	3·580	0·2390	0·00516	0·00334	19·2
35	175	19·0	0·0763	0·0437	62·32	2·465	169	3·05	4·785	6·903	93·02	86·67	1·073	27·96	37·58	3·063	5·09	0·0111	23·44	6·87	0·216	3·491	0·2399	0·00506	0·00319	18·0
36	175	17·0	0·0763	0·0437	62·32	2·465	169	3·05	4·785	6·903	93·02	36·67	1·073	27·96	37·58	3·063	5·09	0·0111	20·97	6·49	0·216	3·297	0·2266	0·00478	0·00291	16·6
37	200	64·5	0·0812	0·0435	62·34	2·569	275	2·89	3·862	7·270	102·8	92·68	1·109	26·70	45·30	3·094	7·16	0·0293	76·35	13·18	0·283	5·327	0·2137	0·00733	0·00602	49·4
38	200	60·5	0·0809	0·0435	62·34	2·569	271	2·90	3·909	7·252	103·0	93·03	1·107	26·96	45·20	3·086	7·01	0·0273	71·62	12·69	0·281	5·175	0·2112	0·00714	0·00582	46·9
39	200	50·5	0·0800	0·0435	62·34	2·569	263	2·92	4·018	7·209	103·7	94·16	1·102	27·60	44·94	3·069	6·68	0·0246	59·78	11·43	0·276	4·746	0·2008	0·00659	0·00522	40·9
40	200	40·5	0·0796	0·0435	62·34	2·569	247	2·95	4·202	7·135	103·6	94·70	1·094	28·67	44·52	3·040	6·17	0·0199	47·94	10·09	0·266	4·346	0·1977	0·00609	0·00466	34·2
41	200	30·5	0·0798	0·0435	62·34	2·569	217	3·02	4·795	6·985	102·1	94·67	1·079	30·87	43·64	2·986	5·30	0·0128	36·11	8·64	0·247	4·010	0·2122	0·00574	0·00417	26·9
42	200	20·5	0·0786	0·0435	62·34	2·569	206	3·06	4·795	6·899	103·0	96·11	1·072	32·13	43·14	2·960	4·89	0·0099	24·27	7·00	0·239	3·356	0·1894	0·00486	0·00321	19·8
43	200	19·0	0·0799	0·0435	62·34	2·569	197	3·08	4·972	6·829	103·4	97·00	1·066	33·16	42·73	2·937	4·59	0·0079	22·49	6·73	0·232	3·316	0·1977	0·00486	0·00313	18·5
44	200	17·0	0·0778	0·0435	62·34	2·569	189	3·11	5·119	6·770	103·2	97·18	1·062	34·03	42·38	2·918	4·35	0·0066	20·12	6·36	0·227	3·212	0·2013	0·00474	0·00296	16·8
45	200	15·0	0·0777	0·0435	62·34	2·569	186	3·12	5·180	6·746	103·2	97·33	1·060	34·38	42·24	2·911	4·26	0·0060	17·76	5·96	0·224	3·043	0·1945	0·00451	0·00270	15·2
46	200	13·0	0·0776	0·0435	62·34	2·569	184	3·13	5·129	6·730	103·1	97·35	1·059	34·61	42·15	2·906	4·20	0·0057	15·39	5·55	0·223	2·850	0·1846	0·00424	0·00241	13·6
47	200	11·0	0·0776	0·0435	62·34	2·569	181	3·14	5·283	6·705	103·1	97·49	1·057	34·99	42·00	2·898	4·11	0·0053	13·02	5·10	0·221	2·648	0·1750	0·00395	0·00209	11·9
48	250	64·5	0·0854	0·0435	62·34	2·569	353	2·93	4·095	7·178	120·9	110·4	1·095	34·99	55·98	2·896	6·09	0·0193	76·35	13·18	0·319	4·732	0·1498	0·00659	0·00545	52·7
49	250	60·5	0·0852	0·0435	62·34	2·569	349	2·94	4·133	7·163	121·0	110·7	1·094	35·26	55·87	2·890	5·99	0·0185	71·62	12·69	0·317	4·589	0·1472	0·00641	0·00525	50·1
50	250	50·5	0·0847	0·0435	62·34	2·569	340	2·96	4·222	7·127	121·4	111·3	1·090	35·91	55·62	2·878	5·77	0·0167	59·78	11·43	0·312	4·198	0·1389	0·00589	0·00471	43·6
51	250	40·5	0·0839	0·0435	62·34	2·569	329	2·98	4·343	7·079	122·0	112·4	1·085	36·80	55·26	2·861	5·49	0·0144	47·94	10·09	0·306	3·780	0·1302	0·00534	0·00412	36·8
52	250	30·5	0·0834	0·0435	62·34	2·569	312	3·01	4·529	7·005	122·2	113·3	1·079	38·16	54·72	2·839	5·11	0·0116	36·11	8·64	0·296	3·340	0·1225	0·00477	0·00349	29·5
53	250	20·5	0·0825	0·0435	62·34	2·569	286	3·06	4·840	6·881	122·4	114·6	1·068	40·43	53·82	2·799	4·54	0·0079	24·27	7·00	0·281	2·852	0·1162	0·00414	0·00277	21·5
54	250	19·0	0·0823	0·0435	62·34	2·569	283	3·07	4·883	6·864	122·6	114·9	1·067	40·75	53·69	2·794	4·47	0·0075	22·49	6·73	0·279	2·760	0·1139	0·00402	0·00263	20·3
55	250	17·0	0·0822	0·0435	62·34	2·569	281	3·08	4·910	6·853	122·6	115·0	1·066	40·95	53·61	2·791	4·43	0·0072	20·12	6·36	0·278	2·618	0·1090	0·00382	0·00242	18·6
56	250	15·0	0·0821	0·0435	62·34	2·569	276	3·09	4·975	6·827	122·6	115·2	1·064	41·43	53·42	2·783	4·33	0·0067	17·76	5·96	0·275	2·483	0·1057	0·00364	0·00221	16·9
57	250	13·0	0·0819	0·0435	62·34	2·569	274	3·09	5·008	6·814	122·8	115·5	1·063	41·67	53·33	2·779	4·28	0·0064	15·39	5·55	0·274	2·231	0·0997	0·00341	0·00197	15·1
58	250	11·0	0·0817	0·0435	62·34	2·569	271	3·10	5·054	6·796	122·9	115·8	1·062	42·01	53·19	2·774	4·21	0·0061	13·02	5·10	0·272	2·150	0·0936	0·00316	0·00171	13·3
59	300	64·5	0·0890	0·0436	62·32	2·499	441	2·96	4·248	7·117	138·3	127·2	1·087	43·16	66·52	2·753	5·45	0·0142	78·49	13·39	0·355	4·205	0·1074	0·00591	0·00489	56·1
60	300	60·5	0·0882	0·0436	62·32	2·499	426	2·98	4·380	7·064	139·8	128·4	1·082	44·32	66·06	2·739	5·18	0·0122	73·63	12·90	0·347	4·135	0·1102	0·00585	0·00480	52·9
61	300	50·5	0·0884	0·0436	62·32	2·499	423	2·99	4·395	7·058	138·6	128·1	1·082	44·45	66·01	2·737	5·14	0·0120	61·46	11·62	0·346	3·739	0·1004	0·00529	0·00424	46·3
62	300	40·5	0·0878	0·0436	62·32	2·499	411	3·01	4·505	7·015	139·2	129·1	1·078	45·42	65·62	2·723	4·93	0·0105	49·29	10·25	0·340	3·357	0·0934	0·00479	0·00370	39·1
63	300	30·5	0·0869	0·0436	62·32	2·499	391	3·04	4·693	6·940	139·8	130·5	1·071	47·06	64·97	2·700	4·58	0·0083	37·12	8·77	0·329	2·960	0·0875	0·00427	0·00313	31·4
64	300	20·5	0·0859	0·0436	62·32	2·499	368	3·08	4·930	6·845	140·6	132·1	1·064	49·15	64·14	2·672	4·20	0·0061	24·95	7·10	0·318	2·488	0·0792	0·00363	0·00243	23·0
65	300	19·0	0·0855	0·0436	62·32	2·499	358	3·09	5·041	6·801	140·8	132·8	1·061	50·12	63·75	2·660	4·04	0·0053	23·12	6·83	0·313	2·433	0·0801	0·00358	0·00234	21·6
66	300	17·0	0·0853	0·0436	62·32	2·499	355	3·10	5·078	6·787	141·0	133·1	1·060	50·45	63·62	2·655	3·99	0·0051	20·69	6·45	0·311	2·310	0·0769	0·00340	0·00216	19·8
67	300	15·0	0·0851	0·0436	62·32	2·499	348	3·12	5·157	6·755	141·1	133·4	1·058	51·14	63·34	2·647	3·88	0·0045	18·25	6·05	0·307	2·194	0·0748	0·00325	0·00198	17·9
68	300	13·0	0·0851	0·0436	62·32	2·499	345	3·12	5·188	6·743	141·0	133·4	1·057	51·42	63·23	2·643	3·84	0·0043	15·82	5·63	0·305	2·052	0·0707	0·00304	0·00177	16·1
69	350	64·5	0·0948	0·0436	62·32	2·499	554	2·95	4·185	7·142	151·5	139·3	1·088	49·65	77·89	2·663	5·38	0·0138	78·49	13·39	0·398	3·745	0·0759	0·00524	0·00437	59·8
70	350	60·5	0·0944	0·0436	62·32	2·499	541	2·97	4·271	7·108	151·7	139·9	1·085	50·53	77·54	2·655	5·20	0·0125	73·63	12·90	0·393	3·658	0·0763	0·00515	0·00425	56·6
71	350	50·5	0·0938	0·0436	62·32	2·499	524	2·99	4·386	7·062	152·3	141·0	1·080	51·70	77·07	2·641	4·97	0·0109	61·46	11·62	0·385	3·358	0·0728	0·00476	0·00383	49·0
72	350	40·5	0·0925	0·0436	62·32	2·499	511	3·01	4·501	7·016	153·8	142·9	1·076	52·89	76·60	2·627	4·74	0·0094	49·29	10·25	0·379	3·011	0·0673	0·00429	0·00334	41·4
73	350	30·5	0·0916	0·0436	62·32	2·499	488	3·04	4·679	6·945	154·7	144·5	1·070	54·71	75·87	2·606	4·43	0·0075	37·12	8·77	0·369	2·648	0·0627	0·00381	0·00282	33·2
74	350	20·5	0·0905	0·0436	62·32	2·499	459	3·08	4·921	6·849	155·5	146·3	1·063	57·20	74·88	2·579	4·06	0·0071	24·95	7·10	0·355	2·227	0·0568	0·00325	0·00220	24·4
75	350	19·0	0·0901	0·0436	62·32	2·499	450	3·09	5·008	6·814	156·1	147·1	1·061	58·09	74·53	2·569	3·93	0·0049	23·12	6·83	0·351	2·168	0·0567	0·00318	0·00211	22·9
76	350	11·0	0·0889	0·0436	62·32	2·499	421	3·14	5·290	6·702	157·0	149·1	1·053	60·99	73·37	2·540	3·57	0·0033	13·39	5·17	0·336	1·713	0·0487	0·00256	0·00142	14·9
77	350	13·0	0·0893	0·0436	62·32	2·499	427	3·13	5·222	6·729	156·6	148·4	1·055	60·29	73·65	2·547	3·65	0·0037	15·82	5·63	0·339	1·846	0·0515	0·00274	0·00162	17·0
78	400	64·5	0·1014	0·0434	62·35	2·605	657	2·95	4·177	7·145	161·8	148·9	1·087	56·84	89·49	2·583	5·22	0·0127	75·30	13·07	0·434	3·496	0·0597	0·00489	0·00412	62·2
79	400	60·5	0·1009	0·0434	62·35	2·605	644	2·96	4·247	7·117	162·2	149·6	1·084	57·67	89·16	2·574	5·07	0·0117	70·63	12·59	0·429	3·408	0·0596	0·00479	0·00400	58·9
80	400	50·5	0·0999	0·0434	62·35	2·605	631	2·98	4·337	7·081	163·4	151·3	1·081	58·74	88·74	2·563	4·89	0·0104	58·96	11·34	0·423	3·110	0·0558	0·00439	0·00359	51·1
81	400	40·5	0·0986	0·0434	62·35	2·605	613	3·00	4·462	7·032	164·9	153·2	1·076	60·20	88·15	2·548	4·65	0·0089	47·28	10·01	0·416	2·796	0·0520	0·00398	0·00314	43·1
82	400	30·5	0·0976	0·0434	62·35	2·605	593	3·02	4·599	6·977	166·1	155·0	1·072	61·82	87·51	2·533	4·42	0·0075	35·61	8·57	0·407	2·443	0·0474	0·00350	0·00264	34·7
83	400	20·5	0·0963	0·0434	62·35	2·605	564	3·06	4·804	6·896	167·5	157·1	1·065	64·23	86·55	2·510	4·09	0·0058	23·93	6·95	0·395	2·042	0·0421	0·00296	0·00206	25·5
84	400	13·0	0·0943	0·0434	62·35	2·605	518	3·12	5·174	6·748	169·5	160·7	1·055	68·61	84·80	2·472	3·59	0·0035	15·18	5·51	0·374	1·708	0·0392	0·00253	0·00155	17·6
85	450	64·5	0·1084	0·0435	62·34	2·569	771	2·94	4·122	7·167	170·4	156·7	1·088	63·02	100·8	2·522	5·19	0·0126	76·35	13·18	0·471	3·205	0·0465	0·00447	0·00378	65·2
86	450	60·5	0·1076	0·0435	62·34	2·569	761	2·95	4·178	7·145	171·3	157·9	1·085	63·76	100·5	2·515	5·07	0·0117	71·62	12·69	0·470	3·112	0·0459	0·00435	0·00366	61·9
87	450	50·5	0·1065	0·0435	62·34	2·569	746	2·96	4·266	7·110	172·7	159·6	1·082	64·93	100·0	2·504	4·89	0·0105	59·78	11·43	0·461	2·838	0·0429	0·00399	0·00328	53·7
88	450	40·5	0·1048	0·0435	62·34	2·569	727	2·99	4·391	7·060	174·9	162·3	1·078	66·57	99·34	2·490	4·65	0·0089	47·94	10·09	0·454	2·546	0·0397	0·00361	0·00287	45·2
89	450	30·5	0·1032	0·0435	62·34	2·569	699	3·01	4·557	6·994	176·6	164·8	1·072	68·78	98·46	2·471	4·36	0·0073	36·11	8·64	0·443	2·233	0·0366	0·00319	0·00242	36·3
90	450	20·5	0·1009	0·0435	62·34	2·569	648	3·07	4·879	6·866	179·2	168·7	1·062	73·05	96·76	2·437	3·87	0·0048	24·27	7·00	0·422	1·897	0·0342	0·00276	0·00193	26·4
91	450	13·0	0·0991	0·0435	62·34	2·569	620	3·11	5·097	6·779	181·6	172·0	1·056	75·94	95·61	2·415	3·59	0·0036	15·39	5·55	0·411	1·547	0·0295	0·00228	0·00141	18·5
92	450	11·0	0·0988	0·0435	62·34	2·569	600	3·13	5·227	6·727	181·7	172·6	1·053	77·67	94·92	2·403	3·43	0·0029	13·02	5·10	0·402	1·452	0·0289	0·00216	0·00126	16·2
93	500	64·5	0·1141	0·0435	62·34	2·569	861	2·95	4·187	7·141	179·3	165·5	1·084	70·92	111·6	2·454	4·92	0·0108	76·35	13·18	0·497	3·038	0·0396	0·00425	0·00362	67·2
94	500	60·5	0·1139	0·0435	62·34	2·569	858	2·95	4·202	7·135	179·6	165·7	1·083	71·13	111·5	2·452	4·89	0·0106	71·62	12·69	0·496	2·932	0·0384	0·00411	0·00347	63·9
95	500	50·5	0·1128	0·0435	62·34	2·569	852	2·96	4·251	7·116	181·1	167·4	1·082	71·86	111·2	2·447	4·79	0·0099	59·78	11·43	0·493	2·654	0·0351	0·00373	0·00305	55·7
96	500	40·5	0·1112	0·0435	62·34	2·569	830	2·98	4·371	7·068	183·1	169·9	1·077	73·62	110·5	3·433	4·57	0·0085	47·94	10·09	0·485	2·382	0·0326	0·00337	0·00270	46·8
97	500	30·5	0·1099	0·0435	62·34	2·569	804	3·01	4·503	7·015	184·5	171·9	1·073	75·57	109·7	2·419	4·34	0·0072	36·11	8·64	0·476	2·079	0·0296	0·00296	0·00227	37·7
98	500	20·5	0·1080	0·0435	62·34	2·569	774	3·04	4·680	6·945	186·9	175·1	1·067	78·17	108·7	2·400	4·06	0·0057	24·27	7·00	0·464	1·726	0·0257	0·00249	0·00176	27·7
99	500	13·0	0·1067	0·0435	62·34	2·569	733	3·07	4·904	6·856	188·2	177·4	1·061	81·48	107·4	2·377	3·74	0·0042	15·39	5·55	0·449	1·415	0·0226	0·00206	0·00130	19·4
100	500	11·0	0·1061	0·0435	62·34	2·569	723	3·09	4·971	6·829	189·0	178·5	1·059	82·47	107·0	2·371	3·65	0·0038	13·02	5·10	0·445	1·313	0·0213	0·00192	0·00115	17·0
101	500	9·0	0·1045	0·0435	62·34	2·569	694	3·12	5·169	6·750	191·0	181·2	1·054	85·40	105·8	2·352	3·41	0·0029	10·65	4·62	0·433	1·219	0·0209	0·00181	0·00099	14·4

In equations (8–13), (dp/dl) is the pressure gradient, r_m the radius of zero shear, r_{01} the core rod radius, r_{02} the tube inside radius, and ρ_G and μ_G the gas density and viscosity. Also, U_1 and U_2 and τ_{01} and τ_{02} are the mean velocities and wall shear stresses for the two regions respectively.

Three further equations are also introduced:

(i) Mass balance:

$$U_1(r_m^2 - r_{01}^2) + U_2(r_{02}^2 - r_m^2) = \bar{U}(r_{02}^2 - r_{01}^2) \qquad (14)$$

where $\bar{U}$ is the mean gas velocity.

(ii) Smooth pipe law for the inner surface; (the Koo equation):

$$F_1 = 0{\cdot}00070 + 0{\cdot}0625(Re_1)^{-0{\cdot}32} \qquad (15)$$

(iii) An equation derived [7] by integration of von Kármán's velocity deficiency law equation, for each region of the annulus:

$$\frac{U_1}{U_2} = \frac{\left[\frac{\sqrt{F_2}}{k}\left\{\frac{r_m + 3\,r_{02}}{2\,r_m + 2\,r_{02}}\right\} + 1\right]}{\left[\frac{\sqrt{F_1}}{k}\left\{\frac{r_m + 3\,r_{01}}{2\,r_m + 2\,r_{01}}\right\} + 1\right]} \qquad (16)$$

k = von Kármán universal constant (taken as 0·368).

With (dp/dl), ρ_G, μ_G, r_{01}, r_{02} and $\bar{U}$ known (as in the present experiments) equations (8–16) can be solved iteratively [7] to yield values of Re_1, Re_2, d_{e1}, d_{e2}, F_1, F_2, U_1, U_2 and r_m respectively. The computer programme was used to perform such an iteration on the present data and the results are tabulated in Table 1 (Columns 9–18). The liquid friction velocity (u^*) on the outer wall was then readily calculated (column 22) and, using also the value of y_i^+ calculated as above, the contact angle, θ, was calculated from equations (1–3). The value of θ was determined for each flow condition at which the pressure drop had been measured. The results are tabulated in Table 1 (column 27) and are plotted in Fig. 6. Each point on this graph represents the theoretical minimum wetting rate (abscissa) for the contact angle given by the ordinate at the gas rate indicated by the legend. As expected, the minimum wetting rate decreases with decreasing contact angle and increasing gas rate. By cross-plotting of Fig. 6, curves of minimum wetting

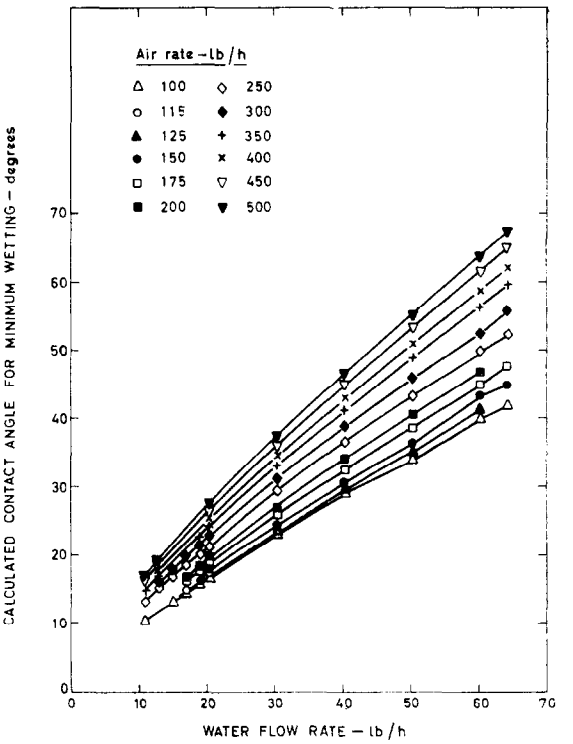

FIG. 6. Calculated contact angles.

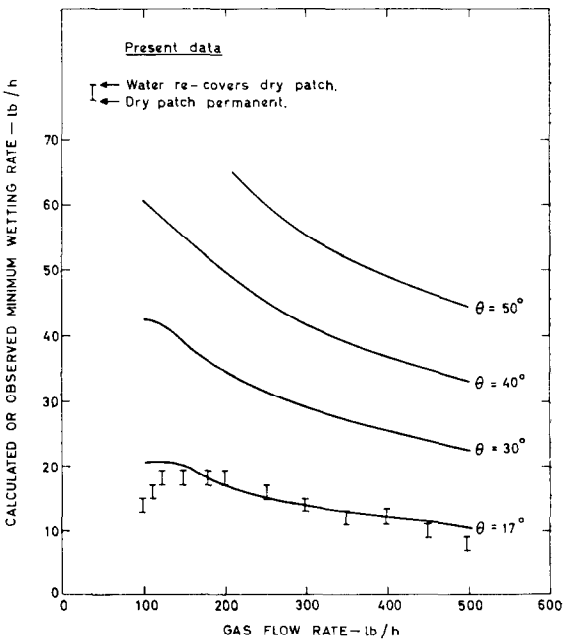

FIG. 7. Comparison of present data with curves for constant contact angle θ.

rate against gas rate can be obtained for constant contact angle, and such curves are plotted in Fig. 7 for contact angles of 50°, 40°, 30° and 17°, i.e. the angles theoretically necessary to cause film breakdown. The value 17° was chosen as giving a curve close to the actual experimental minimum wetting rate data (Fig. 3), which are also plotted in this diagram. The agreement in shape with the curve for a wetting angle of 17° is moderately good; the minimum wetting rate falls below the curve at the lowest and highest gas rates used. The deviation at the lowest gas rate is probably due to the approach to the regime boundary, as discussed above.

It was of interest to obtain a directly determined value of θ for the system water/acrylic-resin-tube/air, and measurements were made using a sessile drop within a short, horizontal section of tube. This was viewed through a rotatable telescope provided with a cross wire which could be aligned with the tube surface or the droplet surface.

The values obtained for θ nearly all lay in the range $49 \pm 4°$; this included new tubing, tubing which had been soaked in water for a long period, and tubing which had been used for air–water experiments over a period of some years. With new tubing, there were occasional spots which had a higher contact angle—presumably as a result of slight greasiness of the surface—but the lowest value obtained in all the tests was 45°.

It is quite probable that the measured static contact angle is not the appropriate one for use in the Hartley–Murgatroyd theory; an advancing edge, however, would experience a larger contact angle than the static one. The theoretical treatment may not, therefore, be valid although it predicts the correct trends. It should be noted that the discrepancy in the forces involved is large, being in the ratio of $(1 - \cos 49°)$ to $(1 - \cos 17°)$, i.e. 7·8:1. The minimum wetting rate is lower than would be predicted from the theory and this suggests the existence of an extra force tending to re-wet the surface. This may possibly take the form of an aerodynamic force on the bulge in the film which occurs immediately below (i.e. upstream of) the dry patch. This "bulge" is caused by the rise in static pressure due to the deceleration of the liquid, and it can be argued that the Hartley–Murgatroyd equations should be derived for this enlarged profile; the equation of motion of the diverging fluid stream would be complex, but to a first approximation the total force resisted by surface forces would be proportional to the maximum thickness of the film at the bulge, which would therefore need to rise by a factor of 7·8 over the film thickness. There is no evidence for such a large increase, and aerodynamic forces on the bulge are likely to provide the largest contribution to the discrepancy.

Much of the analysis depends on the simplifying assumption mentioned earlier, that the shear stress is constant across the liquid film. The validity of this assumption can be tested by comparing the gravitational force on the liquid film ($=m\rho_L g$, where m is the liquid film thickness and g the acceleration due to gravity) with τ_{02}, the interfacial shear stress. m was calculated from y_i^+ and u^*:

$$m = y_i^+ \mu_2 / u^* \rho_L \qquad (17)$$

and values of m and $m\rho_L g/\tau_{02}$ are presented in Table 1 (columns 23 and 24). It will be seen that $m\rho_L g$ is about 50 per cent of τ_{02} at the lowest gas rate (100 lb/h) falling to about 10 per cent at a gas rate of about 250 lb/h and down to about 2 per cent at a gas rate of 500 lb/h. The error in estimating y_i^+ from W^+ is much less than the error in wall shear stress and no attempt has been made to improve the present analysis to take account of the gravity term. Approximate corrections and analyses relating W^+ and y_i^+ are described in reference 9 and a rigorous analytical method is presented in reference 10.

The pressure drop data were of interest in their own right; in a recent report [5], a method was presented for correlating two phase pressure drop data at low liquid rates and high gas rates. The correlation was obtained by plotting calculated roughness height, (ϵ), against "relative film thickness". The relative film thickness (m_r) was the film thickness (calculated) minus the thickness of the laminar sub-layer in the gas phase; this parameter was used by Hartley and Roberts [11]. The data were very well correlated, but only one tube diameter had been used. In the present experiments, the equivalent diameter of the subchannel (see Fig. 5) is not a constant; intuitively, however, one

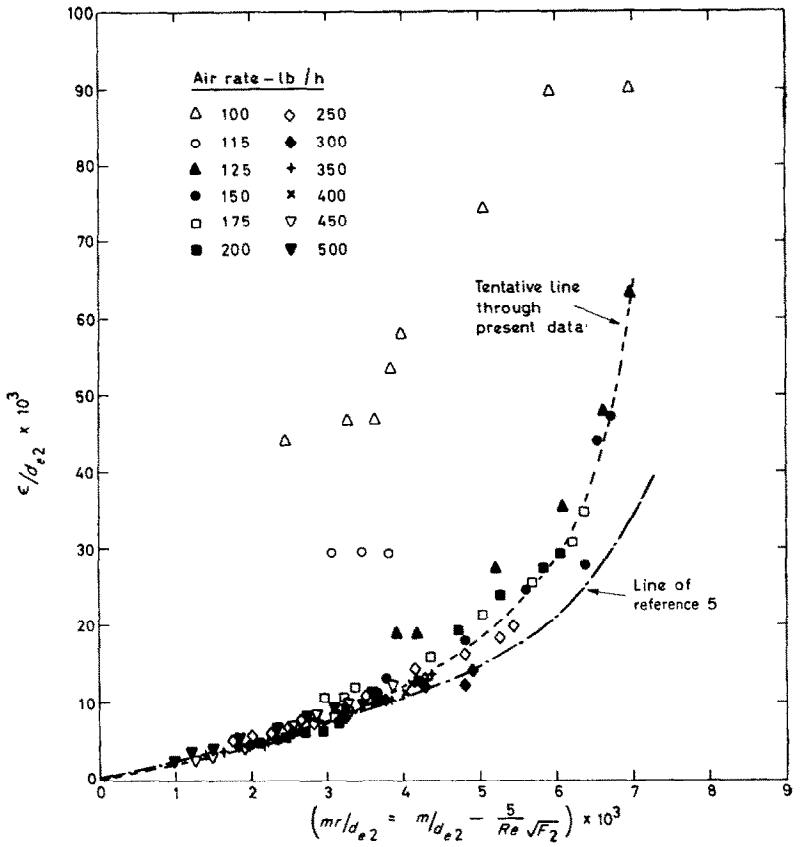

FIG. 8. Relation between relative roughness height and relative film thickness.

might regard it as permissible to divide both the calculated roughness height and the relative film thickness by the equivalent diameter and plot ϵ/d_{e2} against m_r/d_{e2} the latter being given by:

$$m_r/d_{e2} = m/d_{e2} - 5/Re_2\sqrt{F_2} \qquad (18)$$

For convenience, d/e_2 was calculated from the Colebrook–White equation† [12]:

$$\frac{1}{\sqrt{F_2}} = 13{\cdot}02 \ln\left\{\frac{\epsilon/d_{e2}}{3{\cdot}7} + \frac{0{\cdot}887}{Re_2\sqrt{F_2}}\right\} \qquad (19)$$

The results of these calculations are given in Table 1, and ϵ/d_{e2} is plotted against m_r/d_{e2} in Fig. 8. For total air rates above about 150 lb/h the results fall fairly well on to a single curve. (It should be borne in mind that as equation (19) is logarithnic a fairly large error in estimating (ϵ/d_{e2}) gives rise to only a small error in estimating F_2.) The results for air flow rates less than 150 lb/h fall progressively further from the correlating line; this is quite in accord with the results given in reference 5 where data at 100 lb/h (in a $1\frac{1}{4}$ in bore tube) fall well above the line and data at 200 lb/h fell on it.

The correlating line from reference 5 is plotted on Fig. 9; the agreement with the present data for $\epsilon/d_{e2} < 12 \times 10^{-3}$ is encouraging. For greater roughness ratios, the present data lie on a line above that from reference 5. It should be borne in mind, however, that the data on which the reference 5 line was based were extremely

† In the correlation given in reference 5, the gas boundary thickness was calculated as $5/Re\sqrt{(F_G)}$ where F_G is for the smooth pipe. Also, the Nikuradse curve was used for calculating ϵ; this is different from the Colebrook–White curve in the rough–smooth transition region. Neither of the changes made will affect the results seriously.

sparse in this region. Bearing in mind the extent of the transformations required in the present data, the results given in Fig. 9 give confidence in the method of analysis.

5. CONCLUSIONS

The results of the experiments shown above have demonstrated that, at least for higher gas rates, the minimum wetting rate decreases continuously with increasing gas rate. This is in agreement with the trend predicted by Hartley and Murgatroyd but there appears to be a large discrepancy between the contact angle required to satisfy this theory and that measured. This may indicate that there is an important additional force, possibly aerodynamic, which promotes wetting. At lower gas rates, as the regime boundary between climbing film and churn flow is approached, the relationship between minimum wetting rate and gas flow rate reverses.

Spontaneous breakdown of the liquid film from within itself was not observed in any of the present experiments; breakdown at the liquid injector occurred at flow rates about an order of magnitude smaller than the "minimum wetting rate", the latter being the water rate required to re-cover an artificial dry-patch. This result is of importance in burnout considerations; the liquid film will possibly not breakdown when it becomes metastable but evaporation may continue until the film is depleted almost to zero flow. This conclusion assumes, of course, that the heat-transfer process itself cannot provide the initiating force (analogous to the transverse air jet in the present experiment) for breakdown. Breakdown might be started by Marangoni forces as discussed by Norman and McIntyre [13] or by bubble nucleation.

REFERENCES

1. D. E. HARTLEY and W. MURGATROYD, Criteria for the break-up of thin liquid layers flowing isothermally over solid surfaces, Nuclear Research Memorandum *Q5*, Queen Mary College, London (1961). *Int. J. Heat Mass Transfer*, **7**, 1003 (1964).
2. G. F. HEWITT, I. KING and P. C. LOVEGROVE, Techniques for liquid measurements in the two-phase annular flow of air water mixtures, *Brit. Chem. Engng* **8**, 311 (1963).
3. G. F. HEWITT, R. D. KING and P. C. LOVEGROVE, Techniques for liquid film and pressure drop studies in annular two-phase flow. AERE-*R* 3921 (1962).
4. L. E. GILL, G. F. HEWITT, J. W. HITCHON and P. M. C. LACEY, Sampling probe studies of the gas core in annular two-phase flow. Part I. The effect of length on phase and velocity distribution, *Chem. Engng Sci.* **18**, 525–535 (1963); AERE-*R* 3954 (1952).
5. L. E. GILL, G. F. HEWITT and P. M. C. LACEY, Sampling probe studies of the gas core in annular two-phase flow. Part II. Studies of the effect of phase flow rates on phase and velocity distribution, *Chem. Engng Sci.* **19**, 665 (1964). AERE-*R* 3955 (1963).
6. N. HALL TAYLOR, G. F. HEWITT and P. M. C. LACEY, The motion and frequency of large disturbance waves in annular two-phase flow of air–water mixtures. *Chem. Engng Sci.* **18**, 537–552, (1963); AERE-*R* 3952 (1962).
7. G. F. HEWITT, Interpretation of pressure drop data in annular channels. AERE-*R* 4340, H.M. Stationery Office, London (1963).
8. W. B. HALL, Heat transfer in channels composed of rough and smooth surfaces, *J. Mech. Engng Sci.* **4**, (Sept.) 287–291 (1962).
9. J. G. COLLIER and G. F. HEWITT, Data on the vertical flow of air water mixtures in the annular and dispersed flow regions, Part II. Film thickness and entrainment data and analysis of pressure drop measurements, *Trans. Instn Chem. Engrs* **39**, 127 (1961).
10. G. F. HEWITT, Analysis of annular two-phase flow: Application of the Dukler analysis to vertical upward flow in a tube. AERE-*R* 3680 (1961).
11. D. E. HARTLEY and D. C. ROBERTS, A correlation of pressure drop data for two phase annular flows in vertical channels. Nuclear Research Memorandum *Q6*, Queen Mary College, University of London (1961).
12. C. F. COLEBROOK, Turbulent flow in pipes with particular reference to the transition region between smooth and rough pipe lines, *J. Instn Civ. Engrs* **11**, 133 (1936).
13. W. S. NORMAN and V. MCINTYRE, Heat transfer to a liquid film on a vertical surface, *Trans. Instn Chem. Chem. Engrs* **38**, 301 (1960).

Résumé—La disparition des films liquides peut être la cause de la destruction par surchauffe dans les régimes d'écoulement diphasique vapeur d'eau–eau à grande teneur en vapeur d'eau. Une recherche de la disparition du film liquide dans l'écoulement annulaire air–eau est exposée, qui montre que les films peuvent exister dans un état métastable et ne se briseront pas à moins qu'il y ait une perturbation extérieure. Si une telle perturbation est fournie sous la forme d'une tache sèche sur la surface solide, alors de débit minimal d'eau pour lequel la tache sera remouillée diminuera lorsque la vitesse de la phase gazeuse augmente.

Zusammenfassung—Der Zusammenbruch des Flüssigkeitsfilmes kann vielleicht die Ursache für den Burnout in den höheren Qualitätsbereichen eines zweiphasigen Dampf–Wasserstromes sein. Für das Zusammenbrechen eines Flüssigkeitsfilmes in einer Luft–Wasserringströmung wird eine Untersuchung angeführt, die aufzeigt, dass die Filme in einem metastabilen Zustand bestehen können und sich nicht auflösen bis eine Störung von aussen auftritt. Wenn so eine Störung in Form einer trockenen Stelle an der festen Oberfläche vorkommt, dann nimmt die minimale Wasserstromgeschwindigkeit, bei der die Stelle wieder benetzt werden kann, ab unter Geschwindigkeitszunahme der Gasphase.

Аннотация—Разрушение жидких пленок может быть причиной выгорания в более высоких режимах двухфазного потока пар-вода. Проведено исследование разрушения жидкой пленки в кольцевом потоке воздух-вода, которое показывает что пленки могут существовать в метастабильном состоянии и не разрушаться до тех пор, лока нет внешнего возмущения. Если имеется возмущение в виде сухого участка на твердой поверхности, минимальная скорость течения воды, при котором участок будет снова смочен, уменьшается по мере увеличения скорости газовой фазы.